

Organocatalysis

International Edition: DOI: 10.1002/anie.201913563
German Edition: DOI: 10.1002/ange.201913563Peptide-Catalyzed Fragment Couplings that Form Axially Chiral Non- C_2 -Symmetric Biaryls

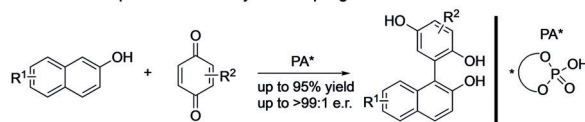
Gavin Coombs, Marcus H. Sak, and Scott J. Miller*

Abstract: We have demonstrated that small, modular, tetrameric peptides featuring the Lewis-basic residue β -dimethylaminoalanine (Dmaa) are capable of atroposelectively coupling naphthols and ester-bearing quinones to yield non- C_2 -symmetric BINOL-type scaffolds with good yields and enantioselectivity. The study culminates in the asymmetric synthesis of backbone-substituted scaffolds similar to 3,3'-disubstituted BINOLs, such as (*R*)-TRIP, with good (94:6 e.r.) to excellent (>99.9:0.1 e.r.) enantioselectivity after recrystallization, and a diastereoselective net arylation of the minimally modified nonsteroidal anti-inflammatory drug (NSAID) naproxen.

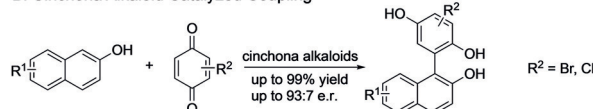
Approaches for the synthesis of enantioenriched biaryl atropisomers are often divided into several categories.^[1] Perhaps the most well-developed method is direct atroposelective coupling of two arene units.^[2] A second method involves a preformed, but stereochemically ambiguous, axis that is kinetically resolved, as pioneered by Bringmann and co-workers,^[3] and for which a number of catalytic examples have now been demonstrated,^[4] including several peptide-catalyzed atroposelective bromination reactions.^[5] Indeed, a burgeoning series of chiral-axis-forming bond constructions exploit a range of chiral catalysis approaches.^[6] Atroposelective biaryl construction through the coupling of one arene to a second partner, which then aromatizes to reveal a newly formed axis of chirality has also been reported.^[7] Recently, our group has contributed to this category with a peptide-catalyzed cyclodehydration that transforms a pre-existing C–N bond into an axis of chirality.^[8] Also within this third category is the innovative work of Tan and co-workers, who demonstrated that BINOL-derived chiral phosphoric acids (BINOL-CPAs), such as (*R*)-TRIP, can catalyze the addition of naphthols to quinones to afford enantioenriched non- C_2 -symmetric biaryls in good yields and selectivity (Scheme 1A).^[9] Complementary to this approach is the excellent work by Salvio, Bella, and co-workers, who showed that cinchona alkaloids were also effective in atroposelectively coupling naphthols to halogenated quinones (Scheme 1B).^[10] Inspired by these studies, and realizing the potential for site- and diastereo-selective arylation of phenol-containing natural products, we wondered whether we could effect a similar

Previous Work

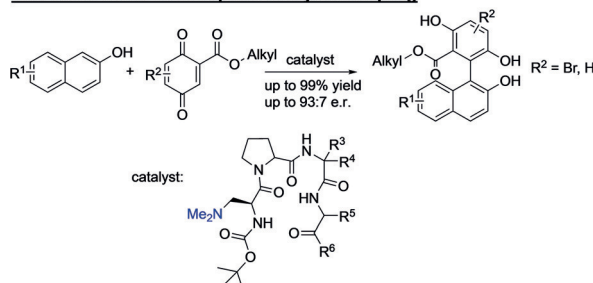
A. Chiral Phosphoric Acid Catalyzed Coupling



B. Cinchona Alkaloid Catalyzed Coupling



This Work: Lewis-Base Peptide-Catalyzed Coupling



Scheme 1. Approaches toward construction of enantioenriched atropisomers through naphthol–quinone coupling.

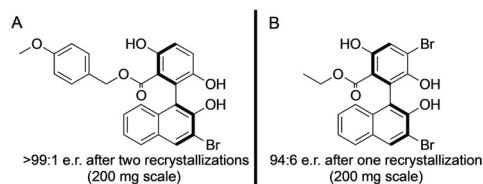
transformation by utilizing a tetrameric peptide featuring a Lewis-basic catalytic residue, as shown in Scheme 1 (bottom). Herein, we present our work on the first peptide-catalyzed,^[11] atroposelective carbon–carbon bond-forming reaction between two independent fragments, an ester-bearing quinone and a naphthol, to yield non- C_2 -symmetric BINOL-type scaffolds.^[12]

Notably, related to the pioneering work of the Tan group and Salvio, Bella, and co-workers,^[9,10] few other examples exist for the organocatalyzed construction of non- C_2 -symmetric BINOL-type catalysts or ligands with substituents decorating the backbone, a feature that often imparts high enantioselectivity.^[13] Important examples include the 3,3'-disubstituted BINOL carboxylic acids developed by Terada and co-workers for hetero-Diels–Alder reactions,^[14] H₈-BINOL-CPAs developed by Krische and co-workers for the enantioselective C–H crotylation of alcohols,^[15] and approaches to preparing racemic NOBIN- and BINOL-type biaryls by Gao et al. and Kamitanaka et al. using quinone monoacetals as coupling partners.^[16]

As we will detail below, these important examples are now complemented by the chemistry presented herein, including the backbone-substituted adducts shown in Scheme 2. We successfully synthesized a highly enantioenriched non- C_2 -

[*] G. Coombs, M. H. Sak, Prof. S. J. Miller
Department of Chemistry, Yale University
225 Prospect Street, New Haven, CT 06511 (USA)
E-mail: scott.miller@yale.edu

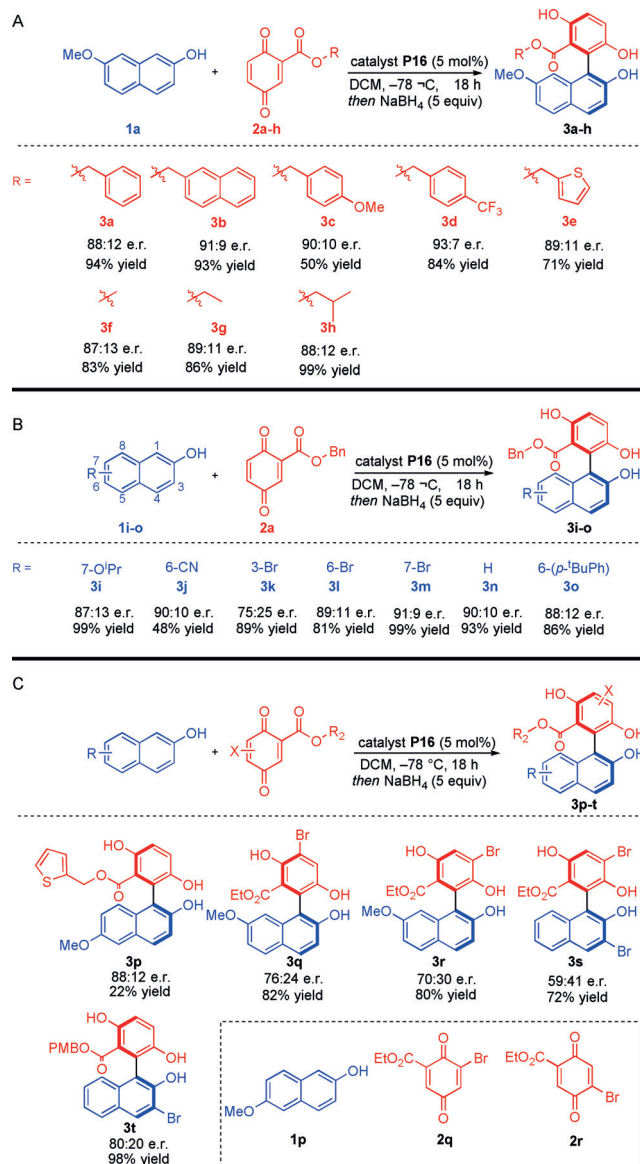
Supporting information (including experimental details) and the ORCID identification number(s) for the author(s) of this article can be found under:
<https://doi.org/10.1002/anie.201913563>.



Scheme 2. Showcase examples of BINOL-type brominated biaryls synthesized through peptide-catalyzed quinone arylation.


symmetric 3-bromo-substituted biaryl (>99.5% *ee* post-recrystallization, Scheme 3 A) and a 3,3'-dibromo-substituted biaryl with good e.r., which affords the opportunity to use them as ligands or for further derivatization. The demonstration that peptide-based catalysts may chaperone highly atroposelective coupling of fragments represents a significant advance for this emerging class of catalysts, with ramifications for complex molecule diversification.

Our investigation commenced with interrogation of a peptide sequence best suited for inducing enantioselectivity in the model reaction shown in Table 1. We believe that the amine on β -dimethylaminoalanine (Dmaa), the catalytic residue, interacts initially with the naphthol –OH group to promote a close interaction between the substrate and catalyst. While the $i+1$ residue is generally a proline of either stereochemistry to encourage the formation of a β -turn through the indicated cross-strand hydrogen bonds,^[17] the amino acids at $i+2$ and $i+3$ are often quite diverse. Positing that an aromatic residue at $i+3$ would enforce potential π – π interactions between catalyst and substrate, we initially evaluated catalysts with a phenylalanine at this position and chose to vary residues at $i+2$ (Table 1, entries 1–5). Our group previously demonstrated in several enantioselective bromination reactions that this position is particularly important in inducing enantioselectivity,^[11e] however in this reaction it proved not to be influential. Replacing phenylalanine with non-aromatic leucine at $i+3$ and exchanging D-proline for L-proline at $i+1$ resulted in significantly lower enantioselectivity (Table 1, entry 6); reinstalling the D-proline residue and adding phenylalanine at $i+2$ in catalyst **P7** did not rescue the enantioselectivity (Table 1, entry 7). We suspected that a tertiary amide at the C-terminus (Table 1, entries 8,9) might enhance the donor capabilities of the $i+3$ carbonyl, thus increasing the strength of the cross-strand hydrogen bond and affording a more rigid solution-phase conformation. Using identical conditions from Table 1, entry 8 but with an additional phenylalanine at $i+2$ (**P9**) resulted in higher yield, but only a marginal decrease in enantioselectivity (Table 1, entry 9). Considering our hypothesis regarding π – π interactions, we incorporated naphthylalanine (Nal; Table 1, entries 10–12) and *O*-benzyltyrosine (Table 1, entry 13) at $i+3$. Retaining the C-terminal dimethylamide (Scheme 4, entries 10–13), we found that **P10** provided the highest enantioselectivity observed thus far with 92:8 e.r. (Table 1, entry 10). Using 2Nal at $i+3$, we again probed the effect that substituents at the C-terminus have on selectivity while varying $i+2$ between aminoisobutyric acid (Aib) and aminocyclopropane carboxylic acid (Acpc; Table 1, entries 14–19). Catalyst **P16**, which had a C-terminal methyl




Scheme 3. Substrate Scope. Yield of isolated product shown; e.r. determined by CSP-HPLC (254 nm, uncorrected). Average of two trials. Absolute configuration shown as (*S*) and assigned in analogy to the data reported by Tan and co-workers^[9] (see Section 6.5 in Supporting Information for details). A) Variations in quinone coupling partner. B) Variations in naphthol coupling partner. Numbering is shown on the naphthol partner for convenience. C) Variations in both coupling partners. Additional coupling partners are boxed. PMB = *p*-methoxybenzyl.

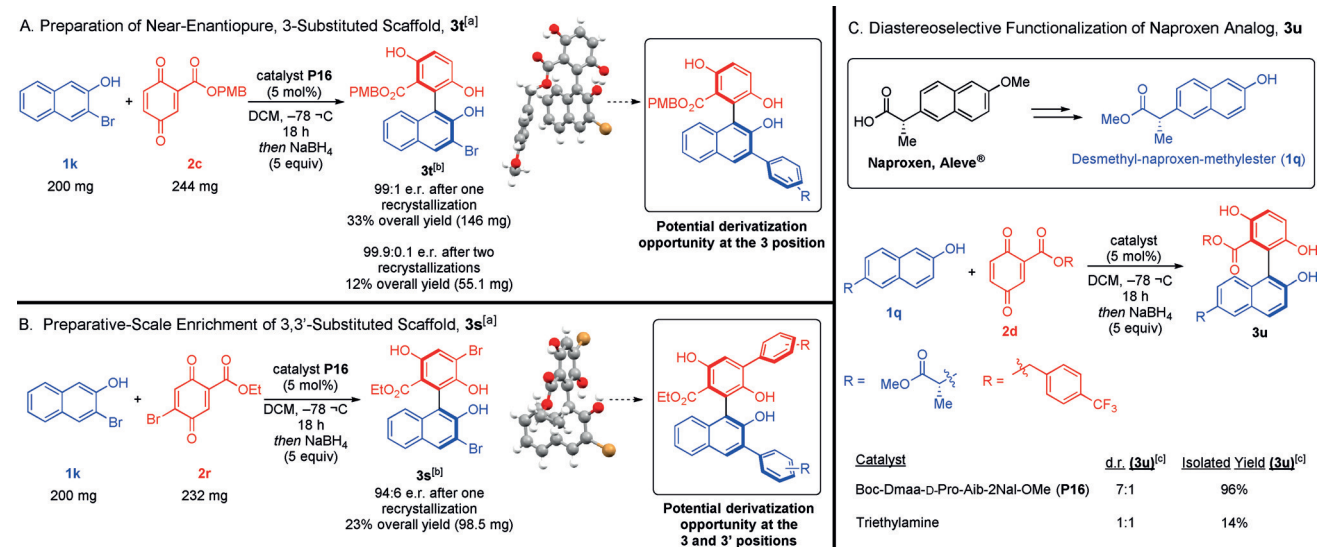
ester, afforded product in similar enantioenrichment as the dimethylamide (**P10**) and diethylamide (**P13**) analogues, but with consistently higher yield over three trials and three hour reaction time. Further attempts to increase the enantioselectivity by incorporating α -methyl valine at $i+2$ (**P19**) failed, as did appending substituents at the 4-position of the proline (**P20** and **P21**). Catalyst **P22** displays a L-proline/*D*-valine-induced β -turn and a chiral C-terminal substituent, which reversed the enantioselectivity (Table 1, entry 23). Interestingly, this reversal is not observed using catalysts **P6** and **P21**,

Table 1: Dmaa^[a] catalyst screen.


Entry	Cat	<i>i</i> + 1	<i>i</i> + 2	<i>i</i> + 3—PG	Yield [%] ^[b]	e.r.	Entry	Cat	<i>i</i> + 1	<i>i</i> + 2	<i>i</i> + 3—PG	Yield [%] ^[b]	e.r.
1	P1	D-Pro	Aib	Phe-OMe	47	88:12	13 ^[c]	P12	D-Pro	Aib	Tyr(Bn)-NMe ₂	53	88:12
2	P2	D-Pro	Acpc	Phe-OMe	51	89:11	14 ^[e]	P13	D-Pro	Aib	2Nal-NEt ₂	62	91:9
3	P3	D-Pro	Gly	Phe-OMe	48	84:16	15	P14	D-Pro	Acpc	2Nal-NMe ₂	92	83:17
4	P4	D-Pro	Ach	Phe-OMe	81	83:17	16	P15	D-Pro	Acpc	2Nal-(<i>R</i>)-αMBA	70	83:17
5	P5	D-Pro	Aic	Phe-OMe	71	82:18	17 ^[f]	P16	D-Pro	Aib	2Nal-OMe	76	92:8
6	P6	L-Pro	Aib	Leu-OMe	65	63:37	18	P17	D-Pro	Acpc	2Nal-NBn ₂	57	74:26
7 ^[c]	P7	D-Pro	Phe	Leu-OMe	51	65:35	19	P18	D-Pro	Aib	2Nal-pyrrolidine	67	85:15
8 ^[c]	P8	D-Pro	Aic	Phe-NMe ₂	54	88:12	20	P19	D-Pro	(αMe)-Val	2Nal-OMe	76	86:14
9 ^[c]	P9	D-Pro	Phe	Phe-NMe ₂	99	84:16	21	P20	D-Pro (4 <i>S</i> -NHCOPh)	Acpc	2Nal-NMe ₂	77	80:20
10	P10	D-Pro	Aib	2Nal-NMe ₂	64	92:8	22	P21	Pro (4 <i>S</i> -NHCOCyMe)	Aib	2Nal-OMe	99	63:37
11 ^[d]	P10	D-Pro	Aib	2Nal-NMe ₂	55	91:9	23 ^[f]	P22	L-Pro	D-Val	2Nal-(<i>R</i>)-αMBA	80	40:60
12 ^[c]	P11	D-Pro	Aib	1Nal-NMe ₂	48	88:12							



A general β-turn catalyst is shown at top left with peptide nomenclature denoted. [a] Boc-Dmaa is the *i*th residue in all catalysts. [b] Yield of isolated product. [c] 2 hour reaction time. [d] 2 hour reaction time, 20 mol% catalyst. [e] Yield and e.r. are the average of two trials. [f] Yield and e.r. are the average of three trials. Uncommon amino acids are highlighted in red within the table and depicted below it.



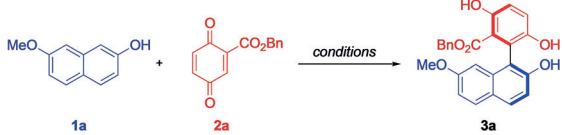
Scheme 4. Applications of this method. [a] 1 equiv of quinone and 1 equiv of naphthol were used in the reaction. Reported e.r. and yields are from one trial). [b] X-ray crystal structures verifying the connectivity of products 3s and 3t (crystallographic data gathered on racemic crystals).^[19] [c] Average of two trials; d.r. determined by ¹H NMR integrations (see Section 7.6 of the Supporting Information).

where L-proline is positioned at *i* + 2 (Table 1, entries 6 and 22).

With optimal catalyst **P16** in hand, we addressed the reaction conditions to increase enantioselectivity and yield. Our standard catalyst screening conditions resulted in the

highest enantioselectivity observed (Table 2, entry 1) but with moderate yield. Increasing the catalyst loading to 10 mol% increased the yield but lowered enantioselectivity (Table 2, entry 2). Further increasing the catalyst loading resulted in decreased enantioselectivity without a substantial change in

Table 2: Conditions Optimization.^[a]



Entry	Solvent	<i>T</i> [°C]	<i>t</i> [h]	Cat. loading ^[b]	Yield [%]	e.r.
1	DCM	−78	3	5	55	93:7
2	DCM	−78	3	10	74	91:9
3	DCM	−78	3	20	64	91:9
4	DCM	−78	3	30	71	89:11
5 ^[c]	DCM	−78	3	30	99	88:12
6 ^[c]	DCM	−78	3	5	99	89:11
7	DCM	−78	24	5	89	90:10
8	DCM	−78	24	2	92	90:10
9 ^[d]	DCM (dry)	−78	24	5	99	88:12
10 ^[d]	CHCl ₃	−60	3	5	99	74:26
11	DCE	rt	3	5	52	50:50
12	DCE	−10	24	5	51	69:31
13	PhMe (dry)	−78	24	5	49	71:29
14	CCl ₄	−10	24	5	52	61:39
15	Et ₂ O	−78	24	5	45	76:24
16	EtCN	−78	16	5	51	93:7
17	MeOH	−78	16	5	8	58:42
18	DCM	−78	18	5	99	89:11

[a] Yield of isolated product. 1 equiv of naphthol and 1 equiv of quinone in DCM (0.06 M in naphthol). NaBH₄ (5 equiv) used in work-up.

[b] Catalyst (**P16**) loading in mol%. [c] DCM (0.02 M in naphthol).

[d] Solvent filtered through basic alumina prior to use.

yield (Table 2, entries 2–4). Running the reaction at a lower concentration markedly improved the yield, perhaps by attenuating side reactivity (Table 2, entries 5,6); however, the enantioenrichment was not restored to the initial result in entry 1. Extended reaction time using 5 mol% catalyst over 24 hours afforded product in good yield but lower selectivity once again (Table 2, entry 7), and lowering the catalyst loading to 2 mol% did not meaningfully alter these results (Table 2, entry 8). Over the course of optimizing the catalyst and the reaction conditions, we were able in some instances to detect by LC–MS the presence of two side products, one originating from oxidation of the desired hydroquinone product (**3**) to quinone, and the other from intramolecular cyclization, presumably leading to a Bringmann-type lactone (see the Supporting Information for details).^[1a,3b] We suspected that perhaps dissolved oxygen in the reaction solvent was responsible for the oxidation and residual acid from dichloromethane was catalyzing the reaction non-selectively or promoting the cyclization. For this reason, we employed anhydrous, degassed dichloromethane that had been filtered through basic alumina prior to use. These efforts, as shown in Table 2, entry 9, did not increase the enantioselectivity, although we were able to isolate product nearly quantitatively after borohydride reduction. In this case, while the formation of lactone was not detected, we still observed the presence of oxidized **3** prior to reductive work up; attempts to isolate this product were unsuccessful. Rather than exogenous oxygen, we propose, in agreement with Salvio and Bella, that in some cases, coupling is followed by rapid oxidation of **3** by **2**.^[10] To

ensure that all coupled material was in the hydroquinone form, we opted to employ a sodium borohydride reduction as a standard procedure in the work-up of all entries in Table 2.

While evaluating other chlorinated solvents, we observed that lower temperatures favored higher enantioselectivity (Table 2, entries 10–12). Toluene provided lower yield and enantioselectivity (Table 2, entry 13), lending support to the proposed productive π – π substrate–catalyst interactions. Similarly, carbon tetrachloride and diethyl ether both furnished the product in lower e.r. and yield (Table 2, entries 14 and 15); however, it should be noted that the solubility of **1a** in these solvents was poor. Despite presenting the opportunity to competitively hydrogen bond with the catalyst, propionitrile afforded desired product in good e.r. albeit with low yield (Table 2, entry 16). With H-bonding donor capabilities, methanol as a solvent resulted in severe depletion of enantioselectivity and yield (Table 2, entry 17). We ultimately chose to pursue the conditions in Table 2, entry 18, which allows the use of more concentrated reaction conditions, no special treatment of the solvent, and slightly reduced reaction time.

Intrigued by the lower selectivity observed when running the reaction in toluene (Table 2, entry 13), we wondered whether appending an extended aromatic system to the quinone substrate would enhance catalyst–substrate recognition (Scheme 3A, **2b**). Indeed, we were able to increase the selectivity slightly relative to our standard benzylester-*p*-quinone coupling partner, **2a**. Investigating a potential correlation between enantioselectivity and electronics on the phenyl group of the quinone, we synthesized more electron-rich quinone **2c** and electron-deficient quinone **2d**. The two substrates gave similar e.r. values, and the trifluoromethyl group afforded the highest e.r. to date at 93:7 e.r. (**3d**). Unfortunately, quinone **2c** was a poor coupling partner in the reaction, and we isolated significant quantities of starting naphthol and hydroquinone after work-up. The reaction is also tolerant of aromatic heterocycles on the quinone coupling partner (**2e**), affording product **3e** in good e.r. In addition, both selectivity and yield remained high when assessing alkoxycarbonyl quinones (**2f–h**).

Variations on the naphthol are also well tolerated (Scheme 3B). The bulky 7-isopropoxy group (**1i**) affected neither the yield nor selectivity, unlike the strongly withdrawing cyano group, which did not affect selectivity, but lowered the yield, perhaps due to decreased nucleophilicity of the naphthol (**3j**). Substitution at the 3-position of the naphthol significantly reduced the enantioselectivity, presumably through sterically inhibiting interactions between the catalyst and the naphthol substrate (**3k**). Appending the bromine to a position more distal from the naphthol –OH restored the enantioselectivity (**3l–m**). Unsubstituted 2-naphthol also performed well in the reaction, retaining good selectivity and yield (**3n**). Investigations into the ramifications of substituents at the 6-position of the naphthol revealed that even sterically encumbered groups, such as 4-*tert*-butyl phenyl (**1o**), do not seriously affect the enantioselectivity or coupling efficiency (**3o**); however, substituting methoxy at this position drastically reduced the reactivity (**1p**). Substituents on the quinone ring itself lowered the enantioselectivity, once

again indicating that perhaps productive catalyst–substrate interactions are inhibited by steric bulk at positions near the phenols on the substrates (**3q**). Product **3r** further corroborates this hypothesis, since placement of the bromine substituent even more proximal to the BINOL-type phenol further reduced enantioselectivity. In the case of 3,3'-disubstitution (**3s**), enantioenrichment is almost entirely ablated. Product **3t** served as a springboard for our foray into preparative scale synthesis and recrystallization of enantioenriched backbone-substituted biaryls, since it produced higher selectivity than the benzylester congener (**3k**).

As shown in Scheme 4A, we succeeded in preparing nearly enantiopure **3t** on a preparative scale after two recrystallizations. It should be noted that significant product enantioenrichment was obtained after only one recrystallization (99:1 er). Furthermore, we were able to obtain **3s** in 94:6 er after one recrystallization (Scheme 4B). We believe these examples represent a significant advancement towards obtaining optically pure scaffolds of this type with the opportunity for myriad diversification, particularly using **3s** to modulate the 3- and 3'-positions of both arenes.^[18]

Concurrently, we explored the possibility of derivatizing a medicinally interesting compound using our catalytic system. To that end, we succeeded in diastereoselectively functionalizing a naproxen analogue, as shown in Scheme 4C. Following minimal modification of naproxen, we obtained **1q**, and under our optimized reaction conditions using quinone **2d** and catalyst **P16**, compound **3u** was afforded in excellent yield with 7:1 d.r.; notable is the lower yield and lack of inherent selectivity when triethylamine is used as a catalyst.

In conclusion, we have demonstrated that a tetrameric peptide featuring a Lewis-basic catalytic residue is capable of efficient and enantioselective fragment coupling to establish an atropisomeric axis. The reaction scope includes backbone-substituted adducts (3- and 3'-positions), as well as the arylation of a naproxen analogue. The intrinsic selectivity may be enhanced by recrystallization, and the products possess handles for myriad functionalizations. The chemistry seems well-poised for appending an appropriately configured bioactive scaffold to either reaction component.

Acknowledgements

The authors are grateful to Aaron L. Featherston, Dr. Anna E. Hurtley, Dr. Anthony J. Metrano, Dr. Jonathan M. Ryss, Dr. Christopher R. Shugrue, and Elizabeth A. Stone for preparation of catalysts. We also acknowledge E.A.S. for invaluable assistance in manuscript preparation. We also thank Dr. Brandon Q. Mercado for solving our X-ray crystal structures, and Dr. Eric K. Paulson for helpful NMR discussions. This work is supported by the National Institute of General Medical Sciences of the National Institutes of Health (R35 GM132092). G.C. acknowledges the support of the NSF Graduate Research Fellowship Program.

Conflict of interest

The authors declare no conflict of interest.

Keywords: atropisomerism · biaryl compounds · organocatalysis · peptides · quinones

How to cite: *Angew. Chem. Int. Ed.* **2020**, *59*, 2875–2880
Angew. Chem. **2020**, *132*, 2897–2902

- [1] a) G. Bringmann, A. J. Price Mortimer, P. A. Keller, M. J. Gresser, J. Garner, M. Breuning, *Angew. Chem. Int. Ed.* **2005**, *44*, 5384–5427; *Angew. Chem.* **2005**, *117*, 5518–5563; b) Y.-B. Wang, B. Tan, *Acc. Chem. Res.* **2018**, *51*, 534–547.
- [2] a) J. Brussee, A. C. A. Jansen, *Tetrahedron Lett.* **1983**, *24*, 3261–3262; b) P. Lloyd-Williams, E. Giralt, *Chem. Soc. Rev.* **2001**, *30*, 145–157; c) J. Hassan, M. Sévignon, C. Gozzi, E. Schulz, M. Lemaire, *Chem. Rev.* **2002**, *102*, 1359–1470; d) T. D. Nelson, R. D. Crouch, *Org. React.* **2004**, *63*, 265–555; e) J. Wencel-Delord, A. Panossian, F. R. Leroux, F. Colobert, *Chem. Soc. Rev.* **2015**, *44*, 3418–3430; f) G. Liao, T. Zhou, Q.-J. Yao, B.-F. Shi, *Chem. Commun.* **2019**, *55*, 8514–8523.
- [3] a) G. Bringmann, M. Breuning, S. Tasler, *Synthesis* **1999**, 525–558; b) G. Bringmann, D. Menche, *Acc. Chem. Res.* **2001**, *34*, 615–624; c) G. Bringmann, M. Breuning, R.-M. Pfeifer, W. A. Schenk, K. Kamikawa, M. Uemura, *J. Organomet. Chem.* **2002**, *661*, 31–47; d) G. Bringmann, S. Tasler, R.-M. Pfeifer, M. Breuning, *J. Organomet. Chem.* **2002**, *661*, 49–65; e) G. Bringmann, H. Scharl, K. Maksimenka, K. Radacki, H. Braunschweig, P. Wich, C. Schmuck, *Eur. J. Org. Chem.* **2006**, 4349–4361.
- [4] a) F. Kakiuchi, P. Le Gendre, A. Yamada, H. Ohtaki, S. Murai, *Tetrahedron: Asymmetry* **2000**, *11*, 2647–2651; b) R. Miyaji, K. Asano, S. Matsubara, *J. Am. Chem. Soc.* **2015**, *137*, 6766–6769; c) C. Yu, H. Huang, X. Li, Y. Zhang, W. Wang, *J. Am. Chem. Soc.* **2016**, *138*, 6956–6959.
- [5] a) J. L. Gustafson, D. Lim, S. J. Miller, *Science* **2010**, *328*, 1251–1255; b) K. T. Barrett, S. J. Miller, *J. Am. Chem. Soc.* **2013**, *135*, 2963–2966; c) M. E. Diener, A. J. Metrano, S. Kusano, S. J. Miller, *J. Am. Chem. Soc.* **2015**, *137*, 12369–12377; d) A. J. Metrano, N. C. Abascal, B. Q. Mercado, E. K. Paulson, S. J. Miller, *Chem. Commun.* **2016**, *52*, 4816–4819.
- [6] B. Zilate, A. Castrogiovanni, C. Sparr, *ACS Catal.* **2018**, *8*, 2981–2988.
- [7] a) J. Bao, W. D. Wulff, M. J. Fumo, E. B. Grant, D. P. Heller, M. C. Whitcomb, S.-M. Yeung, *J. Am. Chem. Soc.* **1996**, *118*, 2166–2181; b) T. Hattori, M. Date, K. Sakurai, N. Morohashi, H. Kosugi, S. Miyano, *Tetrahedron Lett.* **2001**, *42*, 8035–8038; c) A. V. Vorogushin, W. D. Wulff, H.-J. Hansen, *J. Am. Chem. Soc.* **2002**, *124*, 6512–6513; d) J. C. Anderson, J. W. Cran, N. P. King, *Tetrahedron Lett.* **2003**, *44*, 7771–7774; e) T. Shibata, T. Fujimoto, K. Yokota, K. Takagi, *J. Am. Chem. Soc.* **2004**, *126*, 8382–8383; f) Y. Nishii, K. Wakasugi, K. Koga, Y. Tanabe, *J. Am. Chem. Soc.* **2004**, *126*, 5358–5359; g) J. M. Wanjohi, A. Yenesew, J. O. Midiwo, M. Heydenreich, M. G. Peter, M. Dreyer, M. Reichert, G. Bringmann, *Tetrahedron* **2005**, *61*, 2667–2674.
- [8] Y. Kwon, J. Li, J. P. Reid, J. M. Crawford, R. Jacob, M. S. Sigman, F. D. Toste, S. J. Miller, *J. Am. Chem. Soc.* **2019**, *141*, 6698–6705.
- [9] Y.-H. Chen, D.-J. Cheng, J. Zhang, Y. Wang, X.-Y. Liu, B. Tan, *J. Am. Chem. Soc.* **2015**, *137*, 15062–15065.
- [10] M. Moliterno, R. Cari, A. Puglisi, A. Antenucci, C. Sperandio, E. Moretti, A. Di Sabato, R. Salvio, M. Bella, *Angew. Chem. Int. Ed.* **2016**, *55*, 6525–6529; *Angew. Chem.* **2016**, *128*, 6635–6639.
- [11] a) E. A. C. Davie, S. M. Mennen, Y. Xu, S. J. Miller, *Chem. Rev.* **2007**, *107*, 5759–5812; b) H. Wennemers, *Chem. Commun.* **2011**,

- 47, 12036–12041; c) R. C. Wende, P. R. Schreiner, *Green Chem.* **2012**, *14*, 1821–1849; d) K. Akagawa, K. Kudo, *Acc. Chem. Res.* **2017**, *50*, 2429–2439; e) A. J. Metrano, S. J. Miller, *Acc. Chem. Res.* **2019**, *52*, 199–215.
- [12] Peptide catalysis establishing axial chirality: C. T. Mbofana, S. J. Miller, *J. Am. Chem. Soc.* **2014**, *136*, 3285–3292.
- [13] a) P. Kočovský, Š. Vyskočil, M. Smrčina, *Chem. Rev.* **2003**, *103*, 3213–3246; b) M. Shibasaki, S. Matsunaga, *Chem. Soc. Rev.* **2006**, *35*, 269–279.
- [14] N. Momiyama, H. Tabuse, H. Noda, M. Yamanaka, T. Fujinami, K. Yamanishi, A. Izumiseki, K. Funayama, F. Egawa, S. Okada, H. Adachi, M. Terada, *J. Am. Chem. Soc.* **2016**, *138*, 11353–11359.
- [15] J. R. Zbieg, E. Yamaguchi, E. L. McInturff, M. J. Krische, *Science* **2012**, *336*, 324–327.
- [16] a) H. Gao, Q.-L. Xu, C. Keene, M. Yousufuddin, D. H. Ess, L. Kürti, *Angew. Chem. Int. Ed.* **2016**, *55*, 566–571; *Angew. Chem.* **2016**, *128*, 576–581; b) T. Kamitanaka, K. Morimoto, K. Tsuboshima, D. Koseki, H. Takamuro, T. Dohi, Y. Kita, *Angew. Chem. Int. Ed.* **2016**, *55*, 15535–15538; *Angew. Chem.* **2016**, *128*, 15764–15767.
- [17] a) M. W. MacArthur, J. M. Thornton, *J. Mol. Biol.* **1991**, *218*, 397–412; b) T. S. Haque, J. C. Little, S. H. Gellman, *J. Am. Chem. Soc.* **1994**, *116*, 4105–4106; c) T. S. Haque, J. C. Little, S. H. Gellman, *J. Am. Chem. Soc.* **1996**, *118*, 6975–6985; d) H. E. Stanger, S. H. Gellman, *J. Am. Chem. Soc.* **1998**, *120*, 4236–4237; e) S. Rao Raghothama, S. Kumar Awasthi, P. Balaram, *J. Chem. Soc. Perkin Trans. 2* **1998**, 137–144.
- [18] Important examples with scaffolds substituted at the 3- and 3'-positions have also been reported by Bella and co-workers in Ref. [10].
- [19] CCDC 1906659 (**3s**), and 1900403 (**3t**) contain the supplementary crystallographic data for this paper. These data can be obtained free of charge from The Cambridge Crystallographic Data Centre.

Manuscript received: October 23, 2019

Accepted manuscript online: December 2, 2019

Version of record online: December 30, 2019